

Functional histology of the skin in the subterranean African giant mole-rat: Thermal windows are determined solely by pelage characteristics

Lucie Pleštilová¹, Jan Okrouhlík¹, Hynek Burda², Hana Sehadová^{3,4}, Eva Maria Valesky⁵, Radim Šumbera^{Corresp. 1}

¹ Department of Zoology, Faculty of Science, University of South Bohemia, České Budějovice, Czech Republic

² Department of Game Management and Wildlife Biology, Faculty of Forestry and Wood Sciences, Czech University of Life Sciences, Prague, Czech Republic

³ Department of Molecular Biology and Genetics, Faculty of Science, University of South Bohemia, České Budějovice, Czech Republic

⁴ Institute of Entomology, Biology Centre of the Czech Academy of Sciences, České Budějovice, Czech Republic

⁵ Department of Dermatology, Venereology and Allergology, University Hospital, Johann Wolfgang Goethe Universität Frankfurt am Main, Frankfurt am Main, Germany

Corresponding Author: Radim Šumbera
Email address: sumbera@prf.jcu.cz

Excavation of burrows is physically an extremely demanding activity producing large amount of metabolic heat. Dissipation of its surplus is crucial to avoid the risk of overheating, but in subterranean mammals, it is complicated due to absence of remarkable body extremities and high humidity in their burrows. In two species of African mole-rats, it was found by using of IR-thermography that body heat is dissipated mainly through ventral body part, which is remarkably less furred. In our study, we analyzed the skin morphology of the ventral and the dorsal body side, to find if the dermal characteristics could contribute to higher heat dissipation through the ventral body part. Thickness of epidermis and dermis and presence, extent and connectivity of fat tissue in the dermis were examined using routine histological methods, while vascular density was evaluated using fluorescent dye and confocal microscopy in the giant mole-rat *Fukomys mechowii*. Like in other hitherto studied subterranean mammals, no subcutaneous adipose tissue was found. All the examined skin characteristics were very similar for both dorsal and ventral regions: the relative content of adipose tissue in dermis 14.3 ± 4.3 % and 11.4 ± 4.5 %, connectivity of dermal fat 98.6 ± 3.2 % and 94.2 ± 8.3 %, vascular density 26.5 ± 3.3 % and 22.7 ± 2.3 %, respectively. Absence of remarkable differences in measured characteristics between particular body regions indicates that the thermal windows are determined mainly by the pelage characteristics.



Functional histology of the skin in the subterranean African giant mole-rat: Thermal windows are determined solely by pelage characteristics

Lucie Pleštilová¹, Jan Okrouhlík¹, Hynek Burda², Hana Sehadová^{3,4}, Eva Maria Valesky⁵, Radim Šumbera¹

¹ Department of Zoology, Faculty of Science, University of South Bohemia, České Budějovice, Czech Republic

² Department of Game Management and Wildlife Biology, Faculty of Forestry and Wood Sciences, Czech University of Life Sciences, Prague, Czech Republic

³ Department of Molecular Biology and Genetics, Faculty of Science, University of South Bohemia, České Budějovice, Czech Republic

⁴ Institute of Entomology, Biology Centre CAS, v. v. i., České Budějovice, Czech Republic

⁵ Department of Dermatology, Venereology and Allergology, University Hospital, Goethe University Frankfurt, Germany

Corresponding Author:

Radim Šumbera¹

Branišovská 1760, České Budějovice, 37005, Czech Republic

Email address: sumbera@prf.jcu.cz

23 Abstract

24 Excavation of burrows is ~~physically an extremely~~ demanding activity producing large amount of
 25 metabolic heat. Dissipation of its surplus is crucial to avoid the risk of overheating, but in
 26 subterranean mammals, it is complicated due to ~~absence of remarkable~~ body extremities and high
 27 humidity in their burrows. In two species of African mole-rats, it was found by using of IR-
 28 thermography that body heat is dissipated mainly through ventral body part, which is ~~remarkably~~
 29 less furred. In our study, we analyzed the skin morphology ~~of the ventral and the dorsal body~~
 30 ~~side~~, to find if ~~the~~ dermal characteristics could contribute to higher heat dissipation through the
 31 ventral body part. Thickness of epidermis and dermis and presence, extent and connectivity of fat
 32 tissue in the dermis were examined using routine histological methods, while vascular density
 33 was evaluated using fluorescent dye and confocal microscopy in the giant mole-rat *Fukomys*
 34 *mechowii*. Like in other hitherto studied subterranean mammals, no subcutaneous adipose tissue
 35 was found. All the examined skin characteristics were very similar for both dorsal and ventral
 36 regions: the relative content of adipose tissue in dermis $14.3 \pm 4.3 \%$ and $11.4 \pm 4.5 \%$,
 37 connectivity of dermal fat $98.6 \pm 3.2\%$ and $94.2 \pm 8.3\%$, vascular density $26.5 \pm 3.3 \%$ and 22.7
 38 $\pm 2.3 \%$, ~~respectively~~. Absence of ~~remarkable~~ differences in measured characteristics between
 39 particular body regions indicates that the thermal windows are determined mainly by the pelage
 40 characteristics.

41

42 Introduction

43 Mammals are able to maintain stable and relatively high body temperature in a wide range of
 44 ambient temperatures, which is achieved by heat production and heat loss regulation (McNab,
 45 2002; Withers et al., 2016). If they perform energy consuming activity, production of body heat

increases remarkably, yet surplus heat would cause overheating and has to be dissipated (McNab, 2002; Schmidt-Nielsen, 1997; Sherwood, Klandorf & Yancey, 2013). Mammals can lose heat by physical routes i.e. radiation, convection, conduction, or evaporation. Evaporation is the most effective way of cooling, however, it is restricted in water-saturated environment or when water for sweating is not available (Baldo, Antenucci & Luna, 2015; McNab, 2002; Withers et al., 2016).

Heat dissipation in mammals can be enhanced in body areas known as thermal windows (Feldhamer et al., 2015; Withers et al., 2016). These areas are usually sparsely haired and situated at body appendages as pinnae in elephants or rabbits (Mohler & Heath, 1988; Weissenböck et al., 2010), tail in coypus and beavers (Krattenmacher & Rübsamen, 1987; Steen & Steen, 1965), or feet in foxes or otters (Klir & Heath, 1994; Kuhn & Meyer, 2009). Thermal windows are usually well vascularized with numerous arteriovenous anastomoses, regulating the heat transfer by vasodilatation and vasoconstriction (Bryden & Molyneux, 1978; Khamas et al., 2012; Vanhoutte et al., 2002). There are, for example, two main blood vessel plexuses beneath the dark patches of giraffe's skin considered as thermal windows, which facilitates heat exchange with environment (Ackermann, 1976; Mitchell & Skinner, 2004). The blood vessel walls are also thinner in the patches than in non-patch lighter skin (Mitchell & Skinner, 2004). In the proximal region of the wing of the Brazilian free-tailed bat (*Tadarida brasiliensis*), a network of arteries and veins positioned perpendicular to the body was found, which is unique among the bats and which is considered a thermal window allowing effective thermoregulation during migration (Reichard et al., 2010).

Fat layer is due to its low heat conductivity an important component of heat conservation, particularly for aquatic mammals living in cold water (Bryden, 1964; Kvadsheim & Folkow,

1997; Liwanag et al., 2012). These mammals have a thick continuous insulative subcutaneous fat layer all over the body, except for extremities used for active thermoregulation (Khamas et al., 2012; Schmidt-Nielsen, 1997). ~~Isolative~~ properties of fat layer ~~were proven also~~ in much smaller laboratory mice (Kasza et al., 2014, 2016).

Heat dissipation is particularly challenging in burrowing mammals. Digging in mechanically resistant substrate is energetically demanding as it produces a lot of metabolic heat (e.g. Ebensperger & Bozinovic, 2000; Luna & Antenucci, 2007; Lovegrove, 1989; Zelová et al., 2010). We ~~may~~ estimate that ~~especially~~ subterranean mammals (i.e. burrowing mammals, which forage underground) spend several hours per day by digging new burrows and transporting excavated soil. Such activity inevitably produces a surplus of metabolic heat. However, burrow atmosphere is typically very humid (with relative humidity often exceeding 90 %) (reviewed in Burda, Šumbera & Begall, 2007), which impairs the ~~ability~~ of evaporative cooling (Šumbera, 2019). Moreover, subterranean mammals usually lack ~~remarkable~~ body appendages, which would facilitate ~~the~~ heat radiation (see above). ~~Loosing~~ heat via convection in sealed tunnels with very restricted (if any) air currents is also extremely limited (Baldo, Antenucci & Luna, 2015; Burda, Šumbera & Begall, 2007). The best way to dissipate surplus of heat seems to be cooling via conduction through ~~adpressing~~ the body surface to the colder tunnel walls. Indeed, relatively high thermal conductance in subterranean rodents suggests this way of cooling (Buffenstein, 2000).

It was speculated that in subterranean mammals, the ~~body~~ ventral surface is relevant for heat dissipation as indicated by its shorter and less dense fur (Cutrera & Antenucci, 2004; Šumbera et al., 2007). In two species of the African mole-rats (Bathyergidae), the silvery mole-rat *Heliophobius argenteocinereus* and the giant mole-rat *Fukomys mechowii*, importance of the

less furred ventral body side as the main thermal window was supported also by infrared thermography (Šumbera et al., 2007; Okrouhlik et al., 2015). Recently, higher surface temperature of ventral body part in a wide gradient of experimental ambient temperatures was confirmed in other species of subterranean rodents from different phylogenetic lineages (F Vejmelka, 2017, unpublished data).

Morphology of thermal windows in subterranean mammals is heavily understudied. Šumbera et al. (2007) found remarkable differences in pelage between dorsal and ventral body parts in two African mole-rat species. Pelage was four times sparser on belly than on the back in the giant mole-rat and even nine times in the silvery mole-rat. In the later species, hairs on ventral body part were also shorter. Similar differences between ventral and dorsal body regions were found in 15 species of subterranean rodents of different phylogenetic lineages (F Vejmelka, 2015, unpublished data). Importance of fur for heat dissipation has been demonstrated in the South African highveld mole-rat *Cryptomys hottentotus pretoriae* experimentally, because fur shaving decreased body temperature, probably as a result of increased heat dissipation (Boyles et al., 2012). This finding indicates that fur characteristics are probably very relevant for heat dissipation in subterranean species.

Skin morphology of the African mole-rats is rather understudied and the attention was paid mainly to hairless skin of the naked mole-rat (*Heterocephalus glaber*) (Sokolov, 1982; Thigpen, 1940; Tucker, 1981; Daly & Buffenstein, 1998). Later authors compared dorsal skin of *H. glaber* with the common mole-rat (*Cryptomys hottentotus*) and found dense capillary network in the superficial layers of the dermis in the naked mole-rat; unfortunately, situation in furred species was not specified. Kimani (2013) provided a detailed description of skin morphology of different body regions in *H. glaber* and the African root-rat *Tachyoryctes*. He noticed that

thickness of skin is higher on the dorsal side than on the ventral side in both species and explained it by higher resistance to wear during digging. However, the thickness of skin on ventral side is comparable in both species, whereas it is much thicker in *Tachyoryctes* on dorsal side. This difference in the thickness can be caused by presence of fat containing hypodermis on dorsal side of *Tachyoryctes*, which can affect thermoregulation.

In our study, we focus on skin characteristics of the social *F. mechowii*, a species in which the role of ventral body size in heat dissipation has been suggested on the grounds of its higher surface temperatures and lower pelage insulation (Šumbera et al., 2007; Okrouhlík et al., 2015). We focus on comparison of ventral body part (where higher heat dissipation is expected) with the dorsal body side (where heat dissipation should be limited due to the isolating effect of denser fur). There is a question, if heat dissipation on the ventral body part is facilitated due to poor thermal insulation of fur only, or if characteristics of skin also contribute to heat dissipation. If characteristics of skin on ventral body part are relevant for heat dissipation, we may expect lower fat content and connectivity allowing heat exchange through gaps in isolative layer of fat, and also higher vascularization enabling higher heat transport as described in other mammals (Ackermann, 1976; Atlee et al., 1997; Khamas et al., 2012; Mitchell & Skinner, 2004; Reichard et al., 2010).

Materials & Methods

Study animals

The giant mole-rat *Fukomys mechowii* is the largest social African mole-rat with the body mass of 200 g. It is distributed in the Democratic Republic of Congo, Zambia and Angola, where it inhabits mesic savannas, forests, bushlands, and agricultural fields (Kawalika & Burda, 2007;

Wilson, Lacher & Mittermeier, 2017). Animals involved in our study were born in captivity and housed at the temperature 25 ± 1 °C.

We examined skin samples (from dorsal and ventral body sides) of five adult non-breeding females of age 2.5-10 years and body weight 186-308 g. The samples were taken with a biopsy needle (6 mm diameter); in two cases from freshly thawed cadavers stored under -20 °C in three cases, ~~skin samples were harvested~~ from fresh cadavers of animals overdosed by halothane (see below). The material became available when animals were killed for an anatomical study of their brains (Kverková et al. 2018).

Histology

Epidermal and dermal thickness as well as thickness, proportion, connectivity and pattern of dermal fat were assessed in skin samples. From each individual, six skin samples were taken from dorsal and six from ventral body part (see Fig. 1 for details of sampling points). One animal was first processed for analysis of vascularization (see below) and then it was processed by routine histological methods. The other two specimens were sampled from freshly thawed cadavers.

Biopsy samples were fixed in 4% buffered paraformaldehyde (PFA, pH=7.2), dehydrated by ascending concentrations of ethanol in automatic tissue processor (Leica ASP200S) and embedded in paraffin wax in tissue embedder (Leica EG1150H). Paraffin blocks were sectioned on a rotatory microtome (Leica RM2255) to obtain skin cross-sections, which were then mounted on a glass slide and stained with hematoxylin and eosin by an autostainer (Leica XL ST5010). The sections were examined under light microscope (Olympus CX41) with 20× objective magnification and photographed with a digital camera (Olympus DP74).

The micrographs were processed using ImageJ 1.48v (Schindelin et al., 2012). Square grid of side length 300 μm was randomly overlaid over the entire micrograph. Thickness of epidermis, dermis, and dermal fat was measured on 12 random points and respective mean values were calculated. Thickness of epidermis was measured in the direction perpendicular to its border with dermis. Thickness of dermis and fat layer thickness were measured on the internal-external axis of the animal. Dermis was measured from the epidermal junction to the border of the epimysium.

Extent, connectivity and pattern of the dermal fat were established as follows. Square grid of the side length 50 μm was overlaid above the section ~~micrograph and the~~ presence of adipocytes within each grid cell throughout the section was determined and used to calculate the extent of dermal fat as a proportion of grid cells with adipocytes present to the total number of grid cells of the section. To evaluate the dermal fat layer connectivity and pattern we defined seven categories of its thickness based on the total thickness along the internal-external axis – 0, 1-50, 51-100, 100-150, 150-200, 200-250, and >250 μm . Then we divided the section into parts based on the thickness category of fat layer and measured total width of each category on axis parallel with animal surface. We defined fat layer connectivity as a proportion of width of the section including fat tissue to the total section width and we used the fat layer thickness categories as a measure of adipose tissue pattern.

Vascularization density

The vessel system of three females was stained with fluorescent dye by transcardial perfusion as described by Li et al. (2008) and studied by confocal microscopy. In short, animals were perfused with 300 ml of heparinized PBS (pH 7.4) followed by perfusion by 120 ml of lipophilic

carbocyanine dye (solution of 1,1'-dioctadecyl-3,3,3',3'-tetramethylindocarbocyanine perchlorate). Afterwards, the vascular system was perfused with 300 ml 4% buffered PFA. On the next day, skin samples were taken by a biopsy needle and stored in 1% buffered PFA. There were 20 samples per animal in total (see Fig. 1 for details about sampling points). Skin samples were thoroughly rinsed with PBS (four times for 15 min at RT and overnight at 4 °C) and transferred to 100% glycerol through glycerol series (30%, 50%, 80% for 30 min each), mounted on microscope slides and examined under confocal laser scanning microscope (Olympus FV3000) using an objective with 4× magnification (Olympus UPlanSApo4x). Pin-hole size was set automatically to 140 μm, optical filters were set to match ALEXA 568 (i.e. excitation wavelength 561 nm, emission wavelength 603 nm, detection wavelength 570-620 nm), grayscale color depth was 12-bit, other microscope parameters: laser transmissivity 0.30 %, PMT voltage 350 V, gain 1×, offset 2 %, sampling speed 12.5 μs/pixel and resolution 1024×1024. Samples were optically sectioned in Z-axis in 17-20 planes with 30μm distance. Four tiles per plane were imaged and the whole skin sample image in each plane was reconstructed by software stitching (Olympus FV31). To obtain a single plane image with projection of all blood vessels, maximal Z projection of all planes was then performed (ImageJ 1.48v). Contrast of the resulting image was then enhanced using The Curves tool in Gimp [GNU GPL v3+](#) (Solomon, 2009) so that all vessels were clearly visible. For further processing ~~was then~~ the image color resolution reduced to 8-bit. Vessel area and density was then established in the software AngioTool (Zudaire et al., 2011). Vessel density was calculated as proportion (in %) of vessel area to whole area of the sample.

As we did not compare the results statistically, due to a low number of examined individuals, mean values ± SD are given throughout the text and tables unless stated otherwise.

207

208 Results

209 The epidermis of *F. mechowii* consists of 3-10 cell layers covered by a corneous layer. Dermis
210 consists of dense irregular connective tissue with more fibroblasts in papillary layer and regular
211 arrangement of hair follicles in reticular layer (Fig. 2, Fig. 3). Subcutaneous layer (hypodermis)
212 is not clearly delimited and consists of sparse connective tissue, frequently thin and lacking
213 adipocytes. Adipocytes within dermis are rarely present singularly, they usually form clusters of
214 different size and they frequently surrounds growing hair follicles (Fig. 3).

215 Thickness of epidermis, dermis and dermal fat layer thickness for dorsal and ventral skin
216 of each specimens are given in Table 1. Dermal fat layer connectivity was 98.6 ± 3.2 % on dorsal
217 and 94.2 ± 8.3 % on ventral side (Fig. 4). The most represented fat layer thickness category was
218 100-150 μm and the majority of area was occupied by fat layer of thickness 50-200 μm . Detailed
219 proportion of fat layer thickness categories in dermis of each mole-rat is given in Table S1.

220 Mean vessel density counted as proportion of area occupied by vessels inside the
221 maximal projection of whole the explant area (Fig. 5) was 24.6 ± 3.4 % and it was slightly higher
222 on ventral than on dorsal side, 26.5 ± 3.3 % and 22.7 ± 2.3 %, respectively (Fig. 6). Detailed
223 information about each sample is in Table S2.

224

225 Discussion

226 We described skin characteristics such as thickness of epidermis and dermis, relative extent and
227 the pattern of distribution of white adipose tissue in the dermis and vessel density on dorsal and
228 ventral sides of the trunk in the strictly subterranean rodent, the giant mole-rat. All these
229 characteristics were expected to play a role in dissipation of metabolic heat, especially after

energy consuming burrowing, which is typical activity of subterranean mammals. Since we postulate the existence of thermal windows enhancing heat dissipation at the ventral body part of mole-rats, we expected to find morphological differences in skin between ventral and dorsal body parts ~~which would reflect different heat dissipation capabilities~~. Surprisingly, we did not find any remarkable difference between both body surfaces. Although we studied only few individuals (note that evaluation of vessel density requires sacrificing of living animals), the study still provides good insight into the skin structure and its role in heat dissipation in subterranean rodents, a topic that ~~was not~~ studied so far.

The thickness of epidermis and dermis of the giant mole-rat was within the range found by Sokolov (1982) for different rodent taxa including fossorial ones, i.e. 8-80 μm and 0.2-2.8 mm respectively. Sokolov (1982) speculated that ~~scratch-diggers~~ have thicker skin on the breast while ~~chisel-tooth-diggers~~ on the back, as a mechanical protection against wear during digging. Our findings did not confirm this idea, at least for the species under our study, a chisel digger. Thinner epidermis in one individual (# 9653) could be related to older age of this animal compared to the other two individuals, as ~~the epidermal thickness decrease~~ with age ~~as was~~ observed in laboratory mice ~~or human~~ (Bhattacharyya & Thomas, 2004; Branchet et al., 1990; Farage et al., 2007).

Dermal adipose tissue is well developed in many mammalian species; and in rodents, it is clearly separated from the subcutaneous fat tissue by panniculus carnosus (Wojciechowicz et al., 2013; Driskell et al., 2004). Although the dermal fat tissue plays a role in protection and regeneration of skin and hair growth cycle (reviewed in Alexander et al., 2015; Guerrero-Juarez & Plikus, 2018), it also contributes to thermoregulation. Dermal fat layer was found to be thicker in mice facing chronic cold stress and it was calculated, that even ~~only~~ a 200 μm thick layer of

dermal fat prevents heat loss by twofold in mice housed at ambient temperature 16 °C below the body temperature (Kasza et al., 2014, 2016). Dermal adipose tissue forms a continuous layer in the laboratory mouse (Kasza et al., 2014) whereas in the naked mole-rat and in the common mole-rat, this tissue consists of either isolated or grouped adipocytes (Daly & Buffenstein, 1998). In the giant mole-rats, isolated adipocytes are present infrequently, as they form larger clusters situated relatively close to each other, as can be seen from the high connectivity of dermal fat tissue (Fig. 5). The shape of clusters of adipocytes surrounding the hair follicles can be influenced also by the hair cycle as is evident from the Fig. 2 and Fig. 3, and as was described and reviewed in Guerrero-Juarez & Plikus (2011).

Blood vessels play major role in heat exchange, especially in body parts with facilitated heat dissipation (Bryden and Molyneux, 1978; Tarasoff and Fisher, 1970). Our findings showed that relative vessel density is higher on ventral than on dorsal body side, yet the differences are not so prominent (less than 4 %) to cause significant differences in body heat dissipation between both body regions.

In the hitherto studied African mole-rats, no continuous subcutaneous fat layer was found (Daly and Buffenstein, 1998; Sokolov, 1982), while in other mammals, typically, the hypodermis consists mainly of white adipose tissue (Matoltsy, 1986; Marquart-Elbaz et al., 2001; Scudamore, 2014; Sokolov, 1982). Daly and Buffenstein (1998) as well as Sokolov (1982) found only the aggregations of fat cells within the dermis of naked mole-rat and common mole-rat, which is in agreement with our findings. Absence of the subcutaneous fat tissue and thus loose skin connection to the deeper fascia allows the integument slidability, which is known from human anatomy of skin in eyelid or penis (Van De Graaff, 2001). The mobility of loose subcutaneous tissue in subterranean rodents prevents skin from injuries (Kawamata et al., 2003),

which can facilitate movement underground (Daly & Buffenstein, 1998). It is known that instead of storing fat in this layer, at least some African mole-rats (and probably other subterranean mammals) deposit fat into intraperitoneal cavity and around the neck (O’Riain, Jarvis & Faulkes, 1996; Scantlebury, Speakman & Bennett, 2006). Apart from this, absence of subcutaneous fat layer is highly relevant in thermal biology allowing fast heat dissipation of metabolic heat.

We found no remarkable differences in the content and connectivity of dermal fat and vascularization density between the ventral body side, i.e. area with expected heat dissipation function in subterranean rodents (cf. Šumbera et al., 2007; Šumbera, 2019; Cutrera and Antinuchi, 2004) and the dorsal body side. This is in contrast with a prominent difference in the isolative characteristics of fur (hair length and density) between both body areas. In the giant mole-rat, dorsal pelage is four times denser (having the same length), which for sure contributes remarkably to heat conservation (Šumbera et al., 2007). Important role of fur in mole-rat thermoregulation is indicated also by experiments with fur shaving in Mashona mole-rats (*Fukomys darlingi*) and highveld mole-rats (*Cryptomys hottentotus pretoriae*) (Boyles et al., 2012). In mole-rats, heat dissipation could be easily influenced by different pattern of fur characteristics across body together with some behavioral patterns such as curling up and thus hiding the ventral less furred area under cold temperatures. Seasonal changes of microenvironmental conditions in burrows could be faced by seasonal moulting, which is known in some bathyergids (Hislop & Buffenstein, 1994).

Conclusions

If we consider all findings from present study about isolative value of skin and vessel density together with the findings regarding fur (Šumbera et al., 2007), we may conclude that pelage

characteristics are probably the most important factor for dissipation or conservation of body heat in the giant mole-rat. For future studies, focus on potential role of ~~less haired~~ feet or even the short tail on heat dissipation could be interesting. It is known that ~~this body area could~~ also contribute ~~remarkably~~ to heat dissipation, so histological analysis of pads could bring some new information on this issue.

Acknowledgements

We would like to thank Pavel Němec for the transcordial perfusion of three specimens and Matěj Lövy for assistance. We also thank to Monika Doll, Katja Haerle and Jutta Mueller for help with processing of samples.

References

- Ackerman E, 1976. The histogenesis of hair follicles in the zebra and giraffe with special reference to pigmentation and cutaneous vasculature. MSc Dissertation, University of Pretoria, pp 104.
- Alexander CM, Kasza I, Yen CLE, Reeder SB, Hernando D et al., 2015. Dermal white adipose tissue: a new component of the thermogenic response. *Journal of Lipid Research* 56(11): 2061–2069.
- Atlee BA, Stannard AA, Fowler ME, Willemse T, Ihrke PJ, Olivry T, 1997. The histology of normal llama skin. *Veterinary Dermatology* 8: 165–176.
- Baldo MB, Antenucci CD, Luna F, 2015. Effect of ambient temperature on evaporative water loss in the subterranean rodent *Ctenomys talarum*. *Journal of Thermal Biology* 53: 113–118.

322 Bhattacharyya TK, Thomas JR, 2004. Histomorphologic changes in aging skin. Archives of
323 Facial Plastic Surgery 6(1): 21–25.

324 Boyles JG, Verburgt L, McKechnie AE, Bennett NC, 2012. Heterothermy in two mole-rat
325 species subjected to interacting thermoregulatory challenges. Journal of Experimental
326 Zoology 317: 73–82.

327 Branchet MC, Boisnic S, Frances C, Robert AM, 1990. Skin thickness changes in normal aging
328 skin. Gerontology 36(1): 28–35.

329 Bryden MM, 1964. Insulating capacity of the subcutaneous fat of the southern elephant seal.
330 Nature 203: 1299–1300.

331 Bryden MM, Molyneux GS, 1978. Arteriovenous anastomoses in the skin of seals. II. The
332 California sea lion *Zalophus californianus* and the northern fur seal *Callorhinus ursinus*
333 (Pinnipedia: Otariidae). The Anatomical Record 191: 253–260.

334 Buffenstein R, 2000. Ecophysiological responses of subterranean rodents to underground
335 habitats. In: Lacey E, Patton JL, Cameron GN (Eds.), Life Underground: The Biology of
336 Subterranean Rodents. The University of Chicago Press, pp 62–110.

337 Burda H, Šumbera R, Begall S, 2007. Microclimate in burrows of subterranean rodents -
338 revisited. In: Subterranean Rodents: News from Underground. Springer-Verlag, Berlin
339 Heidelberg New York, pp 20–33.

340 Cutrera AP, Antenucci D, 2004. Fur changes in the subterranean rodent *Ctenomys talarum*:
341 Possible thermal compensatory mechanism. Revista Chilena de Historia Natural 77(2): 235–
342 242.

343 Daly J, Buffenstein R, 1998. Skin morphology and its role in thermoregulation in mole-rats,
344 *Heterocephalus glaber* and *Cryptomys hottentotus*. Journal of Anatomy 193: 495–502.

345 Driskell RR, Jahoda CAB, Chuong C-M, Watt FM, Horsley V, 2014. Defining dermal adipose
346 tissue. *Experimental Dermatology* 23: 629–631.

347 Ebensperger LA, Bozinovic F, 2000. Energetics and burrowing behaviour in the semifossorial
348 degu *Octodon degus* (Rodentia: Octodontidae). *Journal of Zoology* 252: 179–186.

349 Farage MA, Miller KW, Elsner P, Maibach HI, 2007. Structural characteristics of the aging skin:
350 A review. *Cutaneous and Ocular Toxicology* 26(4): 343–357.

351 Feldhamer GA, Drickamer LC, Vessey SH, Merritt JF, Krajewski C, 2015. *Mammalogy:*
352 *Adaptation, Diversity, Ecology*. Johns Hopkins University Press, Baltimore, pp 2024.

353 Guerrero-Juarez CF, Plikus MV, 2018. Emerging nonmetabolic functions of skin fat. *Nature*
354 *Reviews Endocrinology* 14(3): 163–173.

355 Hislop MS, Buffenstein R, 1994. Noradrenaline induces nonshivering thermogenesis in both the
356 naked mole-rat (*Heterocephalus glaber*) and the Damara mole-rat (*Cryptomys damarensis*)
357 despite very different modes of thermoregulation. *Journal of Thermal Biology* 19: 25–32.

358 Isola JGMP, Moraes PC, Rahal SC, Machado MRF, 2013. Morfologia, ultraestrutura e
359 morfometria do tegumento da paca (*Cuniculus paca* Linnaeus, 1766) criada em cativeiro.
360 *Pesquisa Veterinária Brasileira* 33(5): 674–682.

361 Kasza I, Suh Y, Wollny D, Clark RJ, Roopra A, Colman RJ, ... & Yen CLE, 2014. Syndecan-1 is
362 required to maintain intradermal fat and prevent cold stress. *PLoS Genet* 10(8): e1004514.
363 doi:10.1371/journal.pgen.1004514.

364 Kasza I, Hernando D, Roldán-Alzate A, Alexander CM, Reeder SB, 2016. Thermogenic
365 profiling using magnetic resonance imaging of dermal and other adipose tissues. *JCI Insight*
366 2016 1(13): e87146.

367 Kawalika M, Burda H, 2007. Giant mole-rats, *Fukomys mechowii*, 13 Years on the stage. In:
 368 Begall S, Burda H, Schleich CE (Eds.) Subterranean Rodents: News from Underground.
 369 Springer-Verlag, Berlin Heidelberg New York, pp 205–219.

370 Kawamata S, Ozawa J, Hashimoto M, Kurose T, Shinohara H, 2003. Structure of the rat
 371 subcutaneous connective tissue in relation to its sliding mechanism. Archives of Histology
 372 and Cytology 66(3): 273–279.

373 Khamas WA, Smolaka H, Leach-Robinson J, Palmer L, 2012. Skin histology and its role in
 374 heat dissipation in three pinniped species. Acta Veterinaria Scandinavica 54: 46.

375 Kimani JM, 2013. Comparative skin morphology and wound healing in Kenyan African mole rat
 376 (*Tachyoryctes ibeanus*) and naked mole rat (*Heterocephalus glaber*). Theses, Department of
 377 Veterinary Anatomy and Physiology, University of Nairobi, Kenya, pp 155.

378 Klir JJ, Heath JE, 1994. Thermoregulatory responses to thermal stimulation of the preoptic
 379 anterior hypothalamus in the red fox (*Vulpes vulpes*). Comparative Biochemistry and
 380 Physiology A 109: 557–566.

381 Krattenmacher R, Rübsamen K, 1987. Thermoregulatory significance of non-evaporative heat
 382 loss from the tail of the coypu (*Myocastor coypus*) and the tammar-wallaby (*Macropus*
 383 *eugenii*). Journal of Thermal Biology 12: 15–18.

384 Kuhn RA, Meyer W, 2009. Infrared thermography of the body surface in the Eurasian otter *Lutra*
 385 *lutra* and the giant otter *Pteronura brasiliensis*. Aquatic biology 6: 143–152.

386 Kvadsheim PH, Folkow LP, 1997. Blubber and flipper heat transfer in harp seals. Acta
 387 Physiologica Scandinavica 161(3): 385–395.

388 Kverková K, Běliková T, Olkiewicz S, Pavelková Z, O’Riain MJ, Šumbera R, ... & Němec P,
389 2018. Sociality does not drive the evolution of large brains in eusocial African mole-rats.
390 Scientific reports 8(1): 9203.

391 Li Y, Song Y, Zhao L, Gaidosh G, Laties AM, Wen R, 2008. Direct labeling and visualization of
392 blood vessels with lipophilic carbocyanine dye DiI. Nature Protocols 3(11): 1703–1708.

393 Liwanag HEM, Berta A, Costa DP, Budge SM, Williams TM, 2012. Morphological and thermal
394 properties of mammalian insulation: the evolutionary transition to blubber in pinnipeds.
395 Biological Journal of the Linnean Society 107(4): 774–787.

396 Lovegrove BG, 1989. The cost of burrowing by the social mole rats (Bathyergidae) *Cryptomys*
397 *damarensis* and *Heterocephalus glaber*: the role of soil moisture. Physiological Zoology 62:
398 449–469.

399 Luna F, Antenucci CD, 2007. Energetics and thermoregulation during digging in the rodent tuco-
400 tuco (*Ctenomys talarum*). Comparative Biochemistry and Physiology, Part A 146: 559–564.

401 Marquart-Elbaz C, Lipsker D, Sick H, Grosshans R, Cribier B, 2001. Does the "subcutaneous
402 cellular tissue" exist? Annales de Dermatologie et de Venereologie 128(11): 1201–1205.

403 Martin AL, Irizarry-Rovira AR, Bevier DE, Glickman LG, Glickman NW, Hullinger RL, 2007.
404 Histology of ferret skin: preweaning to adulthood. Veterinary Dermatology 18: 401–411.

405 Matoltsy AG, 1986. The skin of mammals: Dermis. In: Bereiter-Hahn J, Matoltsy AG, Sylvia
406 Richards K (Eds.) Biology of the integument 2, Vertebrates. Springer, pp 272–277.

407 McNab BK, 1966. The metabolism of fossorial rodents: a study of convergence. Ecology 47:
408 712–733.

409 McNab BK, 2002. The Physiological Ecology of Vertebrates: A View from Energetics. Cornell
410 University Press, New York, 576.

411 Mersmann HJ, Goodman JR, Brown LJ, 1975. Development of swine adipose tissue:
412 morphology and chemical composition. *Journal of Lipid Research* 16: 269–279.

413 Mitchell G, Skinner JD, 2004. Giraffe thermoregulation: A review. *Transactions of the Royal*
414 *Society of South Africa* 59(2): 109–118.

415 Mohler FS, Heath JE, 1988. Comparison of IR thermography and thermocouple measurement of
416 heat loss from rabbit pinna. *American Journal of Physiology* 254(2): R389–R395.

417 O’Riain MJ, Jarvis JUM, Faulkes CG, 1996. A dispersive morph in the naked mole-rat. *Nature*
418 380: 619–621.

419 Okrouhlik J, Burda H, Kunc P, Knížková I, Šumbera R, 2015. Surprisingly low risk of
420 overheating during digging in two subterranean rodents. *Physiology & Behavior* 138: 236–
421 241.

422 Reichard JD, Prajapati SI, Austad SN, Keller C, Kunz TH, 2010. Thermal windows on Brazilian
423 free-tailed bats facilitate thermoregulation during prolonged flight. *Integrative and*
424 *Comparative Biology* 50: 358–370.

425 Scantlebury M, Speakman JR, Bennett NC, 2006. The energy costs of sexual dimorphism in
426 mole-rats are morphological not behavioural. *Proceedings of the Royal Society B-Biological*
427 *Sciences* 273: 57–63.

428 Schindelin J, Arganda-Carreras I, Frise E, Kaynig V, Longair M, Pietzsch T, ... & Tinevez JY,
429 2012. Fiji: an open-source platform for biological-image analysis, *Nature methods* 9(7):
430 676–682.

431 Schmidt-Nielsen K, 1997. *Animal Physiology – Adaptation and Environment*, 5th edition.
432 Cambridge University Press, pp 611.

433 Scudamore CL, 2014. A Practical Guide to the Histology of the Mouse. Wiley Blackwell, pp
434 232.

435 Sherwood L, Klandorf H, Yancey PH, 2013. Animal Physiology: From Genes to Organisms, 2nd
436 edition. Brooks/Cole, pp 816.

437 Sokolov VE, 1982. Mammal Skin. University of California Press, pp 695.

438 Solomon RW, 2009. Free and open source software for the manipulation of digital images.
439 American Journal of Roentgenology 192(6): W330–W334.

440 Steen I, Steen JB, 1965. Thermoregulatory importance of the beaver's tail. Comparative
441 Biochemistry and Physiology A 15: 267–270.

442 Stewart E, Ajao MS, Ihunwo AO, 2013. Histology and ultrastructure of transitional changes in
443 skin morphology in the juvenile and adult four-striped mouse (*Rhabdomys pumilio*).
444 Scientific World Journal, 2013, Article ID 259680.

445 Šumbera R, 2019. Thermal biology of a strictly subterranean mammalian family, the African
446 mole-rats (Bathyergidae, Rodentia) - a review. Journal of Thermal Biology 79: 166–189.

447 Šumbera R, Zelová J, Kunc P, Knížková I, Burda H, 2007. Patterns of surface temperatures in
448 two mole-rats (Bathyergidae) with different social systems as revealed by IR-thermography.
449 Physiology & Behavior 92: 526–532.

450 Tarasoff FJ, Fisher HD, 1970. Anatomy of the hind flippers of two species of seals with
451 reference to thermoregulation. Canadian Journal of Zoology 48(4): 821–829.

452 Thigpen LW, 1940. Histology of the skin of a normally hairless rodent. Journal of Mammalogy
453 21: 449–456.

454 Tucker R, 1981. The digging behaviour and skin differentiations in *Heterocephalus glaber*.
455 Journal of Morphology 168:51–71.

456 Van De Graaff KM, 2001. Human Anatomy, Sixth Edition. McGraw-Hill Publishing Company.

457 Vanhoutte G, Verhoye M, Raman E, Roberts M, Van der Linden A, 2002. In-vivo non-invasive
458 study of the thermoregulatory function of the blood vessels in the rat tail using magnetic
459 resonance angiography. NMR in Biomedicine 15: 263–269.

460 Weissenböck NM, Weiss CM, Schwammer HM, Kratochvil H, 2010. Thermal windows on the
461 body surface of African elephants (*Loxodonta africana*) studied by infrared thermography.
462 Journal of Thermal Biology 35: 182–188.

463 Williams TM, 1990. Heat transfer in elephants: thermal partitioning based on skin temperature
464 profiles. Journal of Zoology 222: 235–245.

465 Wilson DE, Lacher Jr. TE, Mittermeier RA, (Eds.), 2017. Handbook of the Mammals of the
466 World - Volume 7. Rodents II Lynx Editions in association with Conservation International
467 and IUCN, pp 1008.

468 Withers PC, Cooper CE, Maloney SK, Bozinovic F, Cruz-Neto AP, 2016. Ecological and
469 Environmental Physiology of Mammals. Oxford University Press, USA, pp 590.

470 Wojciechowicz K, Gledhill K, Ambler CA, Manning CB, Jahoda CAB, 2013. Development of
471 the mouse dermal adipose layer occurs independently of subcutaneous adipose tissue and is
472 marked by restricted early expression of FABP4. PLoS One 8(3): e59811.
473 doi:10.1371/journal.pone.0059811.

474 Wright PG, 1984. Why do elephants flap their ears? South African Journal of Zoology 19: 266–
475 269.

476 Zelová J, Šumbera R, Okrouhlik J, Burda H, 2010. Cost of digging is determined by intrinsic
477 factors rather than by substrate quality in two subterranean rodent species. Physiology &
478 Behavior 99: 54–58.

479 Zudaire E, Gambardella L, Kurcz C, Vermeren S, 2011. A computational tool for quantitative
 480 analysis of vascular networks. PLoS ONE 6(11): e27385.

481

Figure 1

Schematic location of skin sampling points on the animal.

A – sampling points for evaluation of the area covered by vessels, B – sampling points for routine histological evaluation of epidermis, dermis and fat tissue characteristics. Samples were taken from both dorsal and ventral body side.

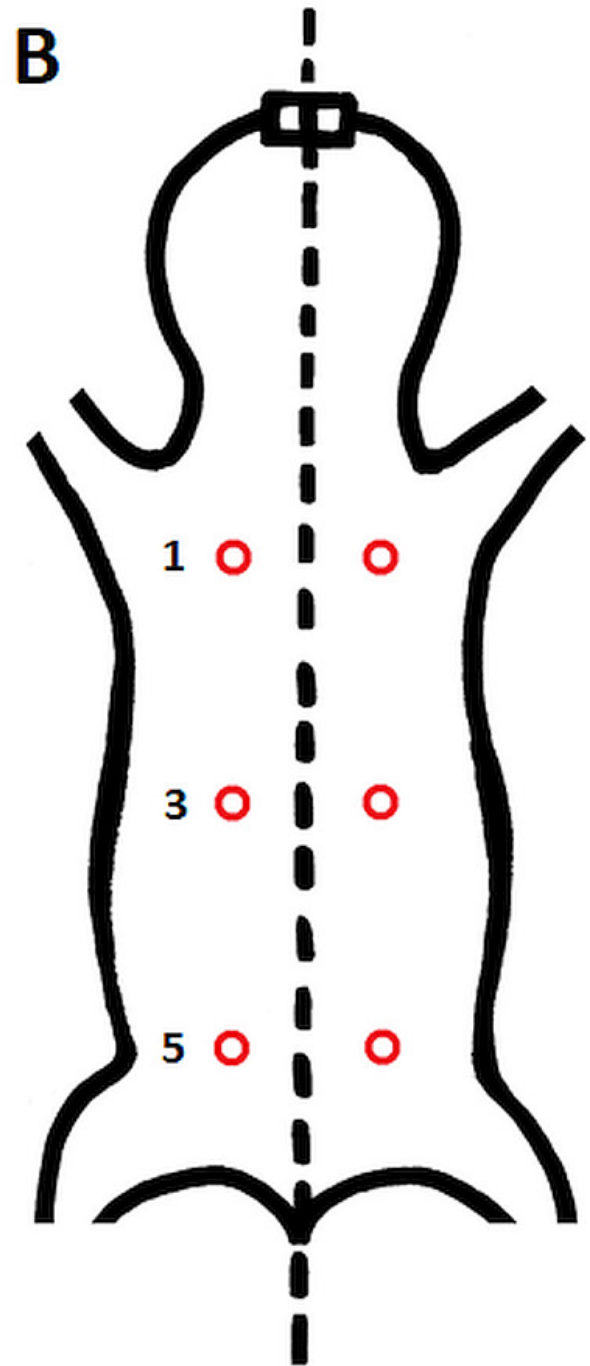
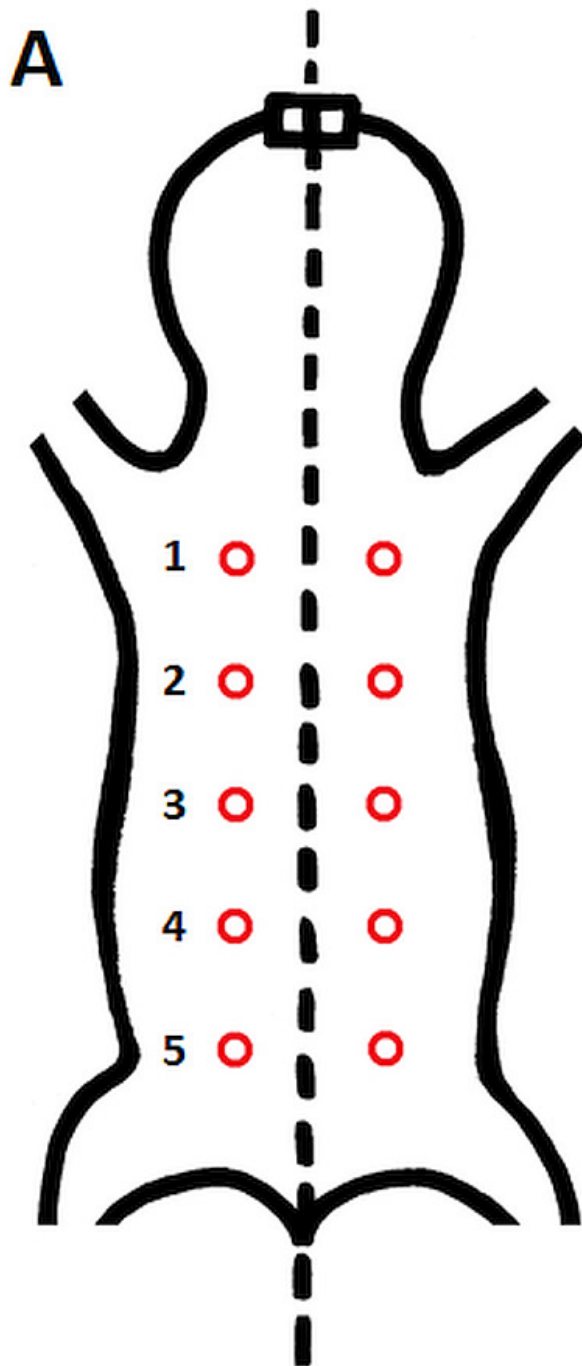


Figure 2

Histological section of skin in *Fukomys mechowii*.

The section of thickness 4 μm was stained by hematoxylin and eosin, D - dermis, E - epidermis, M - muscle layer, A -adipose tissue.

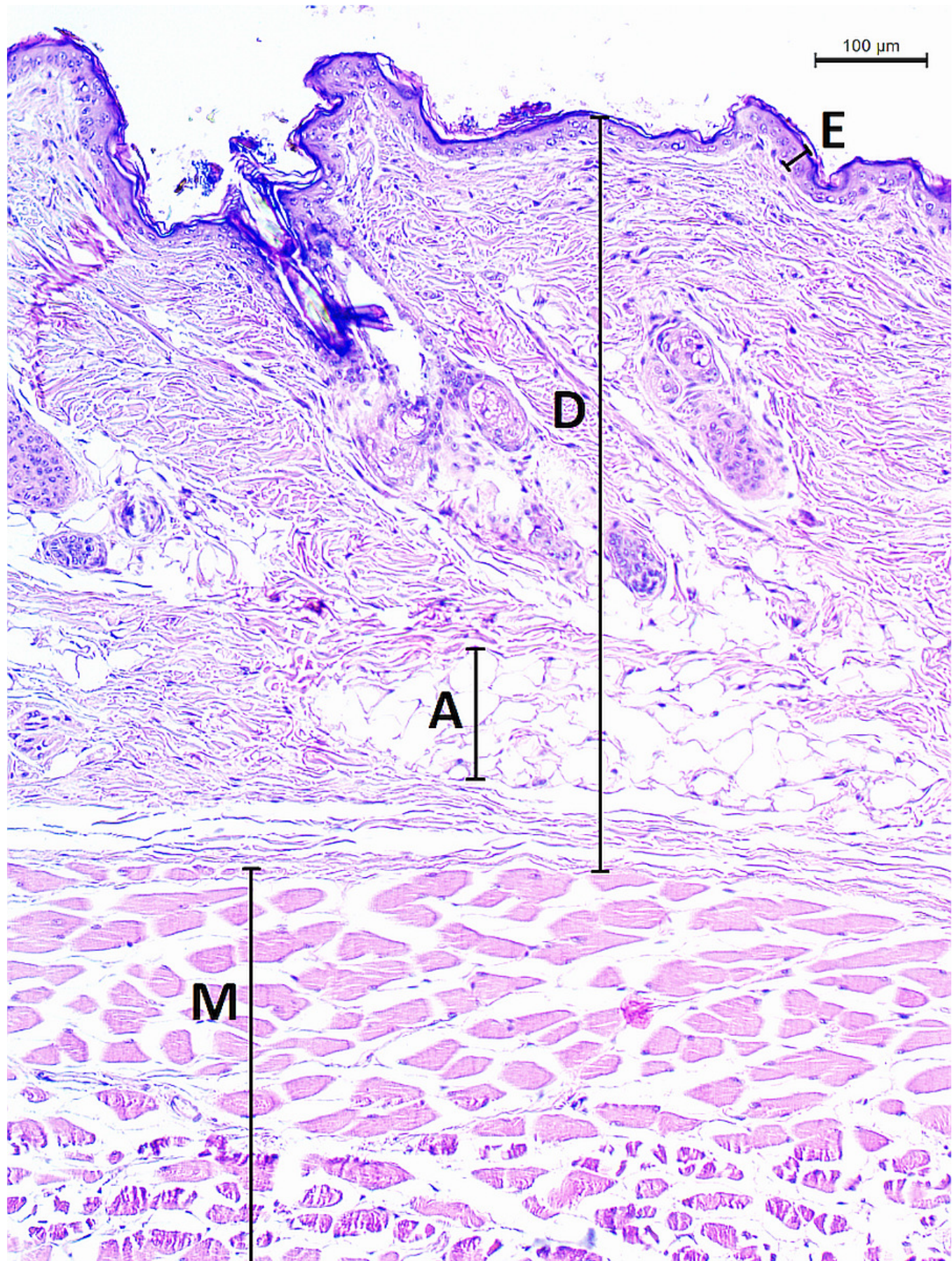


Figure 3

Histological section of skin in *Fukomys mechowii* showing distribution of adipocytes surrounding hair follicles.

The section of thickness 4 μm was stained by hematoxylin and eosin. A – adipocytes, HF – hair follicles with associated glands, M – muscle.

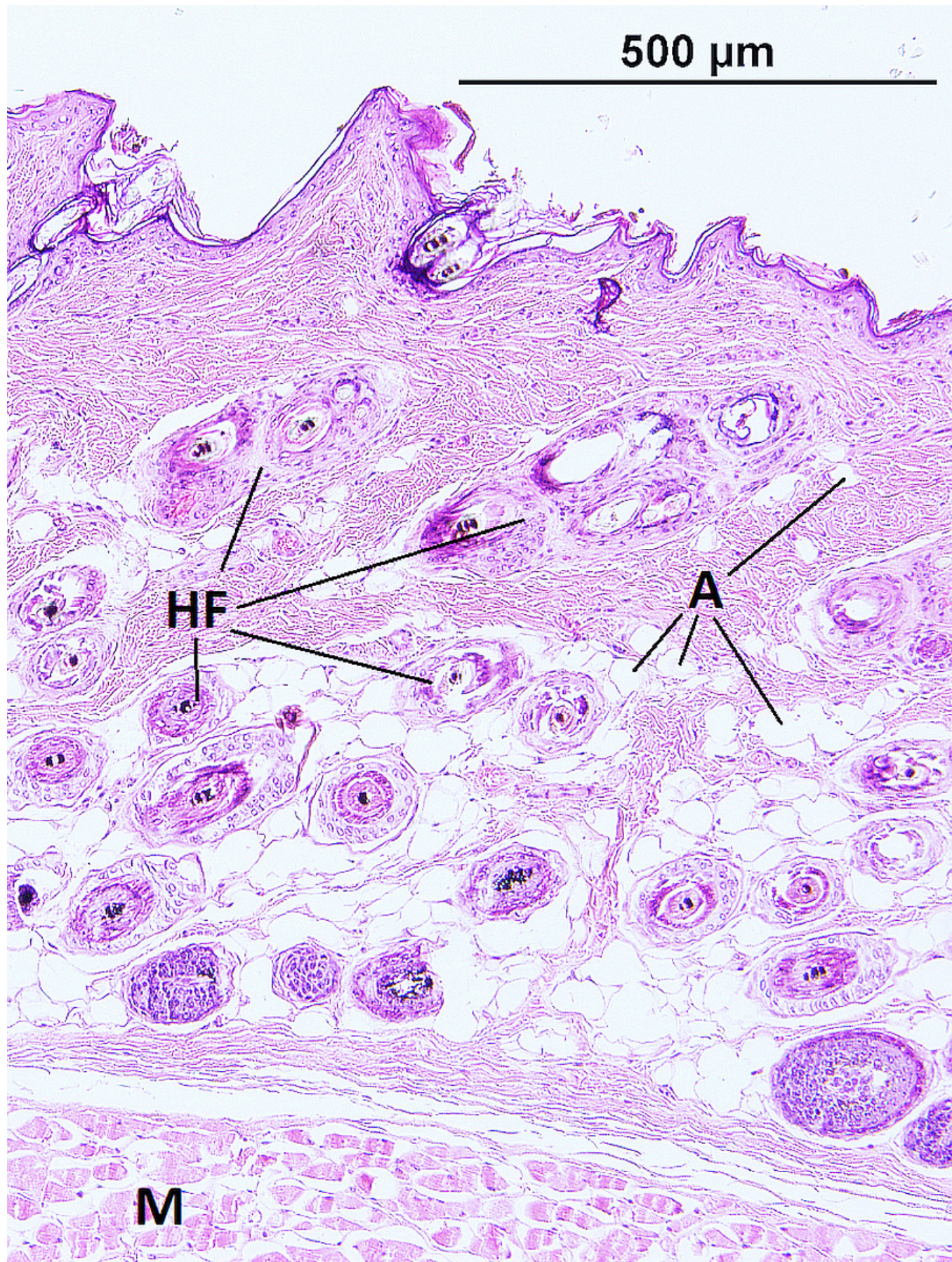


Figure 4

Dermal fat tissue connectivity in *Fukomys mechowii*.

Proportion of skin sample width containing any dermal fat tissue. Boxplots showing medians (horizontal lines), quartiles (boxes), 5 and 95 percentiles (whiskers) and outliers (black dots) for each animal. Numbers above denote animal ID, D - dorsal and V - ventral body side.

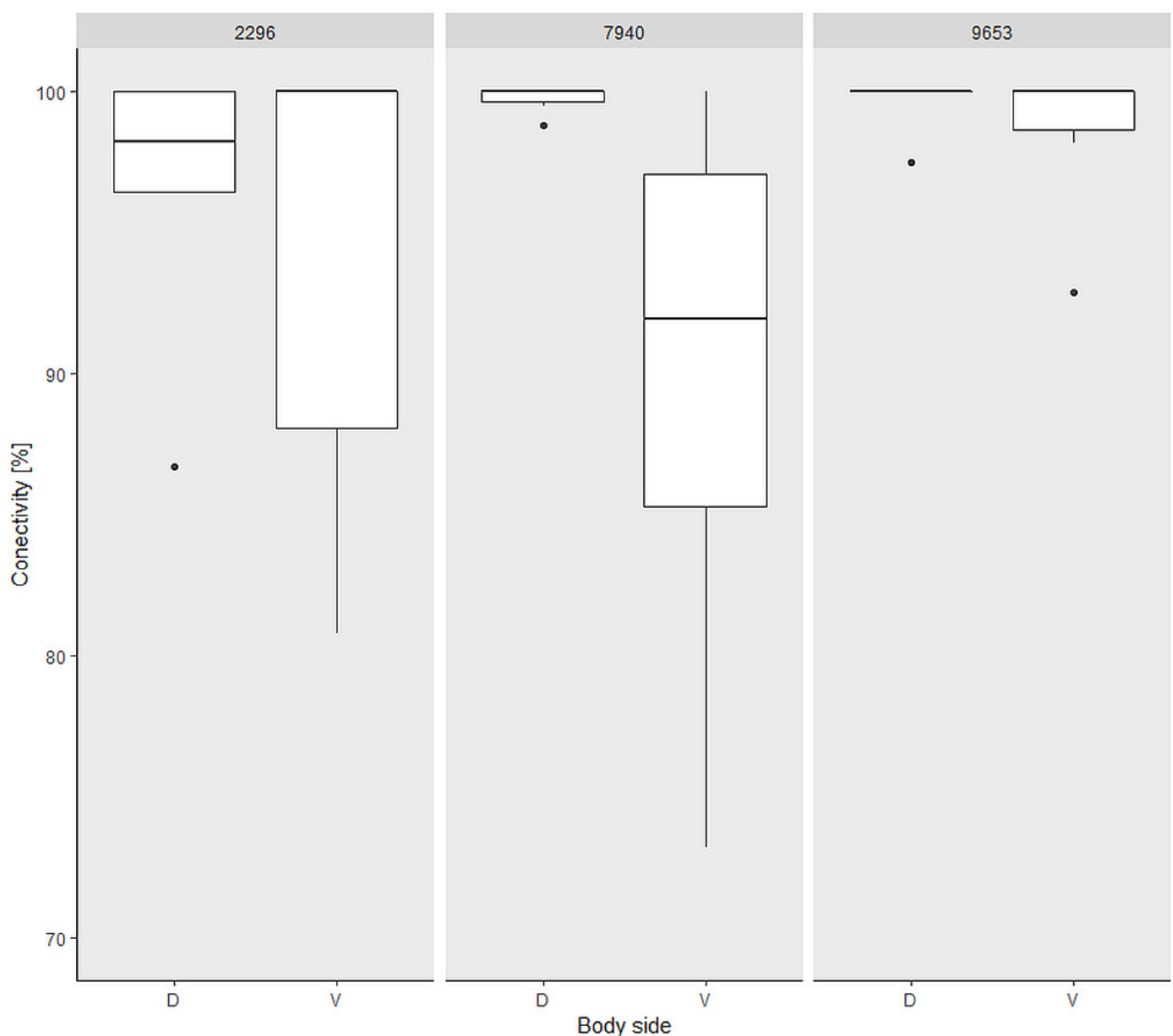


Figure 5

Blood vessels of *Fukomys mechowii*.

Visualized by Dil labeling, enhanced maximal projection of 17 planes with 30µm distance viewed by confocal microscope.

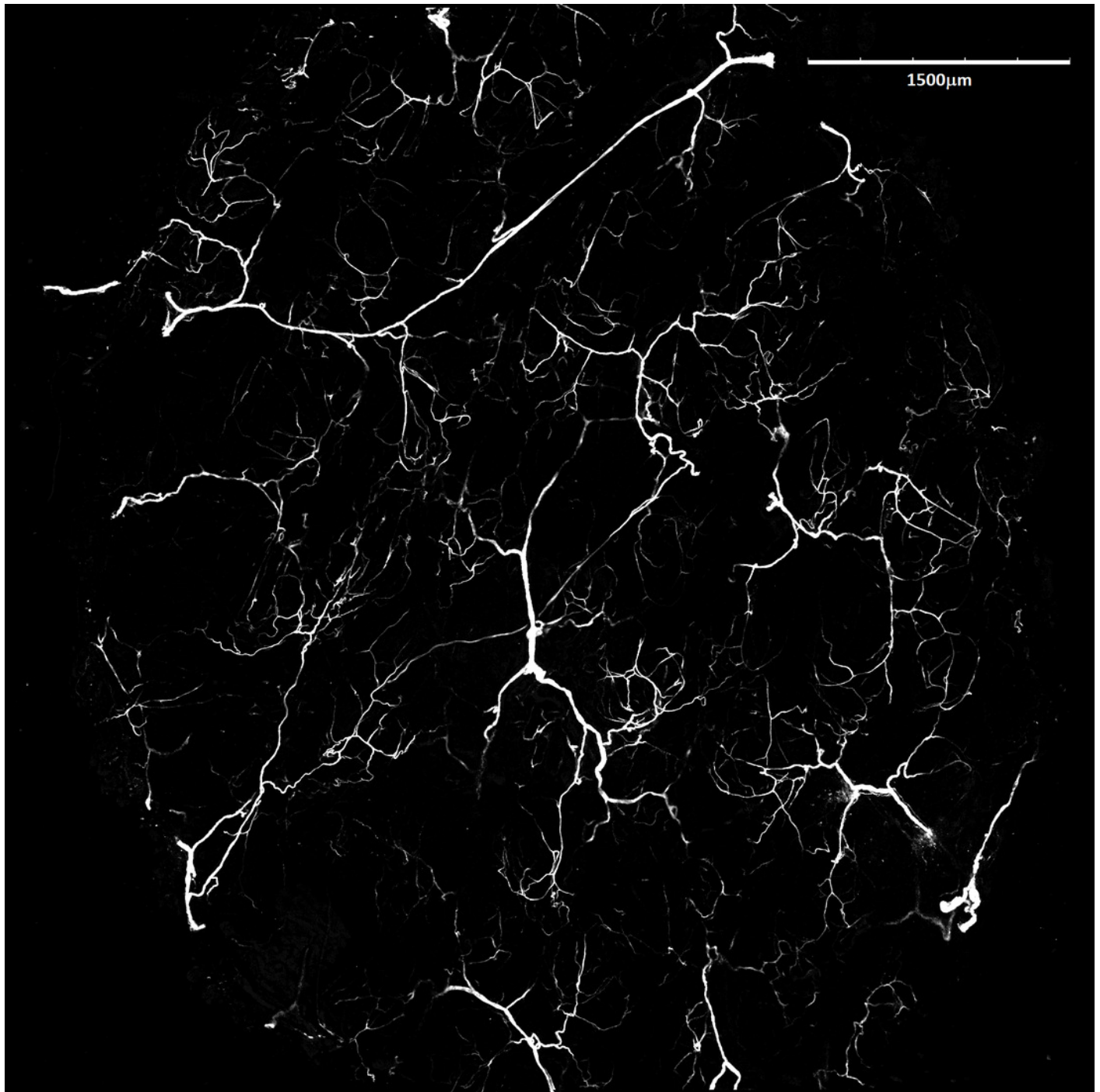


Figure 6

Vascular density in *Fukomys mechowii*.

Percentage of area covered by vessels in maximal projection of whole skin sample. Boxplots showing medians (horizontal lines), quartiles (boxes), 5 and 95 percentiles (whiskers) and outlier (black dot) in each animal. Numbers above denote animal ID, D - dorsal and V - ventral body side.

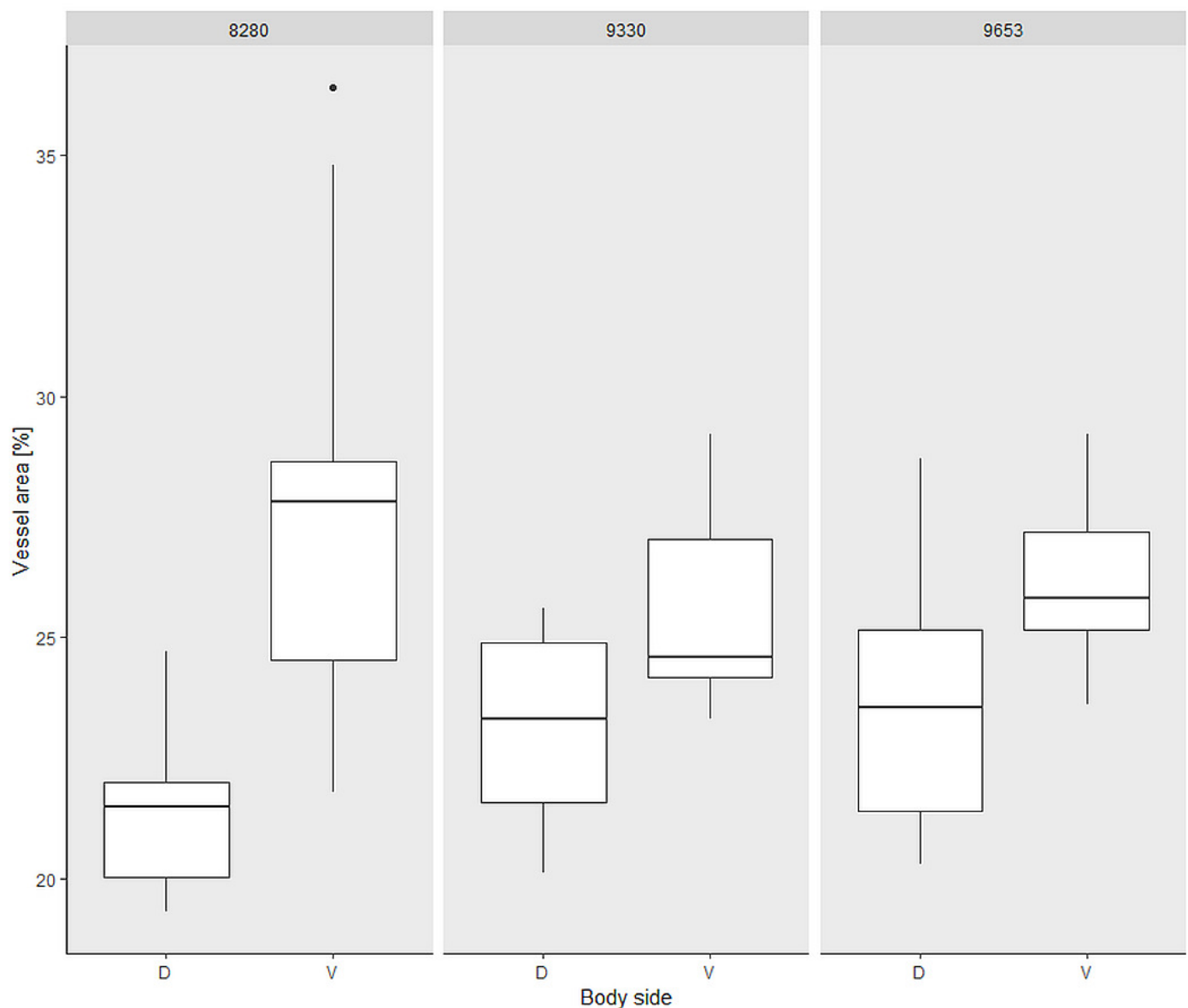


Table 1(on next page)

Skin characteristics on dorsal and ventral body part in three females of *Fukomys mechowii*.

Mean \pm SD of epidermis, dermis, and fat tissue thickness and proportion of fat tissue in dermis for dorsal and ventral side of each animal.

1

Animal ID	Body mass (g)	Age (years)	Epidermis (μm)		Dermis (mm)		Fat layer (mm)		Fat (%)	
			Dorsum	Venter	Dorsum	Venter	Dorsum	Venter	Dorsum	Venter
2296	187	2.5	19.4 ± 6.0	21.6 ± 7.5	0.7 ± 0.2	0.9 ± 0.2	0.1 ± 0.1	0.2 ± 0.1	14.3 ± 2.8	12.1 ± 3.3
7940	186	2.75	20.3 ± 8.2	19.6 ± 8.6	1.0 ± 0.2	1.0 ± 0.3	0.2 ± 0.1	0.1 ± 0.1	10.8 ± 3.1	8.1 ± 3.8
9653	290	10	10.8 ± 4.8	14.0 ± 5.9	0.7 ± 0.2	0.7 ± 0.2	0.2 ± 0.1	0.2 ± 0.1	17.8 ± 4.2	14.1 ± 4.6
Mean	221 ± 60	5±4	16.3 ± 7.7	17.6 ± 7.9	0.8 ± 0.2	0.8 ± 0.3	0.2 ± 0.1	0.2 ± 0.1	14.3 ± 4.3	11.4 ± 4.5

2